

Ab Initio Calculation of ^{17}O NMR Parameters of Tricluster Oxygen Sites in Borosilicate Glasses

Y. Yoneyama¹, M. Urushihara¹, S. Sakida², T. Nanba¹, Y. Miura¹

¹Department of Environmental Chemistry and Materials, Okayama University,
3-1-1, Tsushima-Naka, Okayama, 700-8530, Japan.

²Health and Environment Center, Okayama University,
3-1-1, Tsushima-Naka, Okayama, 700-8530, Japan.

Keywords: borosilicate glass, tricluster oxygen, molecular orbital calculation, NMR parameter

Abstract

^{17}O NMR parameters of the tricluster oxygen atoms in borosilicate system were theoretically predicted by means of molecular orbital calculations. Various cluster models containing tricluster oxygen atoms were constructed. In the cluster models prepared from borate crystals, the tricluster oxygen atoms surrounded by tetrahedral boron atoms (B[4]) were in a similar isotropic chemical shift δ_i^{O} compared to the bridging oxygen atoms in B[4]–O–B[4] bridges. In quadrupole coupling constant C_Q and asymmetry parameter η , the tricluster oxygen atoms were different from the bridging oxygen atoms. Significant difference was also observed in ^{17}O MQMAS NMR chemical shifts. The chemical shift in isotropic dimension was almost the same, but that in MAS dimension was different. The tricluster oxygen atoms appeared at the lower frequency region in MAS dimension. The cluster models were also constructed by the geometry optimization of molecular orbital calculations. In the cluster models containing the larger numbers of Si and trigonal B[3] atoms, the ^{17}O MQMAS NMR peaks of the tricluster oxygen atoms appeared at the same region with those of the bridging oxygen atoms in B[4]–O–B[4] bridges. It was finally concluded that only the tricluster oxygen atoms surrounded by tetrahedral B[4] atoms were identified by ^{17}O MQMAS NMR, if present in glass.

Introduction

It has been widely accepted that in aluminosilicate glasses, non-bridging oxygen (NBO) atoms disappear at the equivalent point of $\text{Na}_2\text{O}/\text{Al}_2\text{O}_3 = 1$. In borosilicate glasses, it has been commonly accepted that NBOs are not present at $\text{Na}_2\text{O}/\text{B}_2\text{O}_3 < 1/2$ [1]. According to the recent ^{17}O NMR analyses [2,3], however, NBOs were confirmed even in the glasses where NBOs should not be produced, and it was also proposed that tricluster oxygen (TO) was responsible for the formation of NBO. In oxide glasses, oxygen atoms are generally classified into two groups, that is, BO (bridging oxygen) and NBO. BOs are coordinated by two network forming (NWF) atoms such as B, Si, Ge, P and tetrahedral Al, and NBOs are bound to only one NWF. TO is surrounded by three NWFs. Tetrahedral $\text{BO}_{4/2}$ and $\text{AlO}_{4/2}$ units possess a unit negative charge, and hence charge compensators such as alkali and alkali-earth network modifying (NWM) cations are required for charge neutrality. In the tricluster units containing tetrahedral B or Al atoms, however, less or no NWM cations are needed, because the negative charges of the BO_4 and AlO_4 units are reduced. For example, $(\text{O}_{3/2}\text{Si})\text{O}(\text{BO}_{3/2})_2$ tricluster unit carries a unit negative charge, and hence only one alkali cation is enough to compensate the charge of tricluster unit. The unused alkali cation is consumed to form an NBO at another place.

The presence of NBOs is confirmed from various experiments, but the direct evidence for the presence

of TOs has never been reported. As for aluminosilicate glasses, molecular orbital calculations have been performed to predict the ^{17}O NMR parameters, and the TOs have been identified by means of NMR spectroscopy [4,5]. However, the predicted NMR parameters of TOs were quite similar to those of BOs, and hence the experimental identification of TOs might be impossible.

In borosilicate glasses, the presence of TOs has been proposed based on the ^{17}O NMR analysis [3]. However, to the best of the authors' knowledge, theoretical predictions of NMR parameters have never been reported. Nanba et al. [6,7] have studied the structure of borosilicate glasses based on the various experimental observations, such as XPS and NMR spectroscopy. They have also performed molecular orbital calculations to discuss the chemical bonding character of borosilicate glasses [8]. Recently, Urushihara et al. [9] have carried out molecular orbital calculations to evaluate the ^{17}O NMR chemical shifts of various oxygen sites in borosilicate glass. In the present study, the ^{17}O NMR parameters of tricluster oxygen atoms in the borosilicate system were predicted by means of molecular orbital calculations.

Experimental

Cluster Models

In the present study, cluster models were constructed with two methods; TOs are found in borate crystals, such as high pressure form of B_2O_3 ($\text{B}_2\text{O}_3\text{-II}$) [10] and SrB_4O_7 [11], and hence cluster models were constructed from the TO-containing borate crystals. Among the borosilicate crystals, however, no crystal was found in which TOs were present. Then, various cluster models containing SiO_4 , BO_3 and BO_4 units were constructed, and the atomic arrangement was optimized by using molecular orbital calculations.

As shown in Figure 1, various cluster models containing TOs were constructed from the borate crystals. The cluster model shown in Figs. 1(a) and 1(b) were constructed from $\text{B}_2\text{O}_3\text{-II}$, in which tricluster oxygen atom was placed at the center of the clusters. In every cluster model, hydrogen atoms were located 0.057 nm apart from the terminal oxygen atoms in the direction toward the next atoms. When the terminal oxygen was tricluster oxygen, the terminal tricluster oxygen should be terminated by up to two H atoms (addressed as +2H) according to the present rule. In this study, cluster models terminated by the reduced number of H atoms (addressed as +1H) were also prepared. In the case of the clusters constructed from SrB_4O_7 (Figs. 1(c) and 1(d)), cluster models containing charge compensating Na ions instead of Sr ions were also prepared (Fig. 1(d)). For comparison, clusters in dimeric forms including $\text{B}[4]\text{-O-B}[4]$, $\text{B}[4]\text{-O-B}[3]$ and $\text{B}[3]\text{-O-B}[3]$ bridges are also constructed from the crystals of SrB_4O_7 and $\text{Na}_2\text{B}_4\text{O}_7$ [12].

Various cluster models containing tricluster oxygen atoms were constructed, and geometry optimizations were performed by using the Gaussian03 program [13]. In most models, however, bond dissociation or recombination took place, and originally-intended structures could not be obtained. Then, the bond lengths of $\text{TO-B}[3]$, $\text{TO-B}[4]$ and $\text{TO-Si}[4]$ and angles between these bonds were fixed at appropriate values, and structural optimizations were executed again. In this way, tricluster models with various combinations among BO_3 , BO_4 and SiO_4 units were obtained.

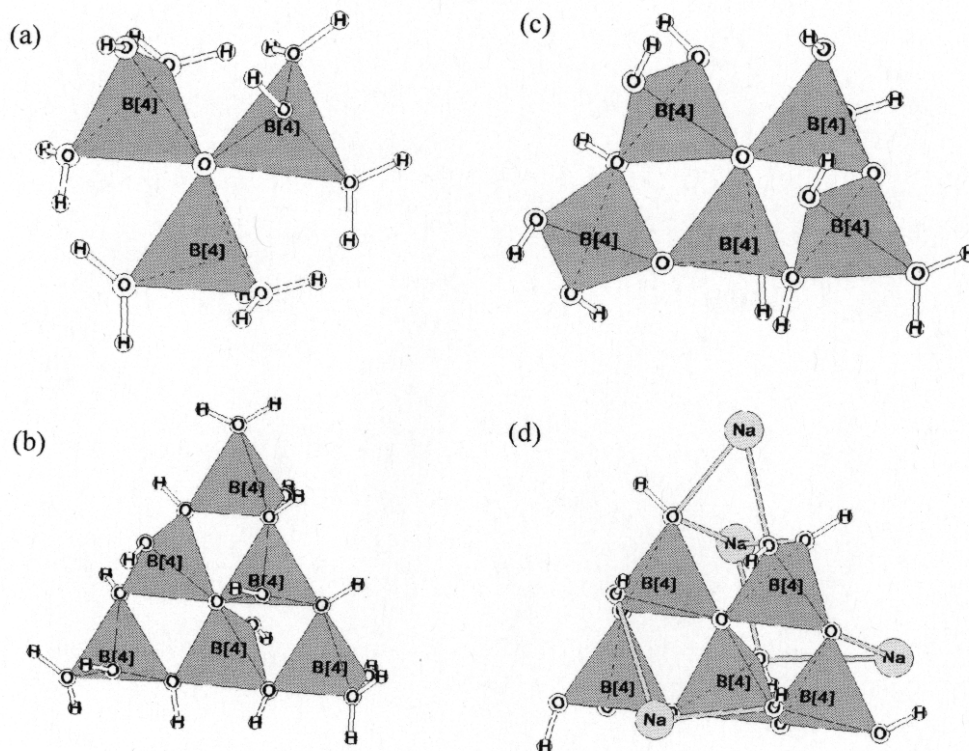


Figure 1: Cluster models including tricluster oxygen atoms surrounded by three tetrahedral boron atoms B[4], TO(B[4]₃), prepared from borate crystals of B₂O₃-II (a, b) and SrB₄O₇ (c, d).

Computation

After obtaining the optimal geometry, NMR parameter calculations were carried out with HF/6-311+G(2df,p) basis by using the Gaussian03 program. In the magnetic shielding tensor calculations, the Gauge-Independent Atomic Orbital (GIAO) method [14] was used. The isotropic chemical shifts of oxygen, δ_i^O (in ppm) were estimated from the following equation:

$$\delta_i^O(\text{cluster}) = \sigma_i^O(\text{H}_2\text{O}) - \sigma_i^O(\text{cluster}) \quad (1)$$

where σ_i^O is the ¹⁷O isotropic magnetic shielding (in ppm) obtained from MO calculations. H₂O cluster was geometrically optimized using HF/3-21G(d), and the referential σ_i^O was obtained with HF/6-311+G(2df,p).

The ¹⁷O quadrupole coupling constant, C_Q was calculated using the following equation:

$$C_Q = e^2 q_{zz} Q / h \quad (2)$$

where eQ is the quadrupole moment of the objective oxygen and the experimental value for H₂O molecule (10.175 MHz) [4,15]. The term, eq_{zz}, is the largest absolute value of the electric field gradient (EFG) tensor at the nucleus in the principal axis.

Asymmetry parameter, η was calculated according to:

$$\eta = (eq_{xx} - eq_{yy}) / eq_{zz} \quad (3)$$

Peak position in ^{17}O MQMAS NMR spectra is reproduced from the chemical shifts of δ_{iso} and δ_{MAS} in isotropic and MAS dimensions, respectively, according to the following equations [16]:

$$\delta_{\text{iso}} = -\left(\frac{17}{31}\right)\delta_{\text{iso}}^{\text{CS}} + \left(\frac{10}{31}\right)\delta_{\text{iso}}^{2\text{Q}} \quad \delta_{\text{MAS}} = \delta_{\text{iso}}^{\text{CS}} + \delta_{\text{iso}}^{2\text{Q}} \quad (4)$$

where $\delta_{\text{iso}}^{\text{CS}}$ is the isotropic chemical shift given in Eq. 1, and $\delta_{\text{iso}}^{2\text{Q}}$ is the second-order quadrupolar shift given by:

$$\delta_{\text{iso}}^{2\text{Q}} = -\frac{3 \times 10^6}{40} \frac{[I(I+1)-3/4]}{I^2(2I-1)^2} \left[\frac{C_Q^2(1+\eta^2/3)}{\nu_0^2} \right] \quad (5)$$

where ν_0 is the NMR frequency [MHz], I is the nuclear spin ($^{17}\text{O} = 5/2$), η is the asymmetry parameter given in Eq. 3, and C_Q is the quadrupole coupling constant given in Eq. 2.

Results and Discussion

^{17}O NMR Parameters for Tricluster Oxygen in Borate Crystals

^{17}O NMR chemical shifts δ_i^{O} which are obtained from the cluster models constructed from borate crystals are shown in Figure 2. As for TOs, only the results of the central TO atoms are indicated in Fig. 2. In the cluster formed by three BO_4 units (Fig. 1(a)), there is no difference in δ_i^{O} between the models having the different numbers of terminal hydrogen atoms, +2H and +1H. In the larger clusters (Fig. 1(b) ~ (c)), however, significant differences were confirmed between the models, +2H and +1H, but the difference is less than 10 ppm. Between the clusters associated with and without Na ions, difference in δ_i^{O} is observed, however, it is not so large.

In Fig. 2, δ_i^{O} of bridging oxygen atoms in $\text{B}[4]\text{--O--B}[4]$ bridges ($\text{BO}(\text{B}[4],\text{B}[4])$) are also indicated, which are almost the same value with those of TOs. As shown in Figs. 1(c) and 1(d), TOs and BOs are in a trimeric ring, suggesting some effects of the trimeric rings. As for BOs in the simple dimers, BOs in $\text{B}[4]\text{--O--B}[4]$ bridges show the different δ_i^{O} with those in the trimeric rings, also implying the trimeric ring effects.

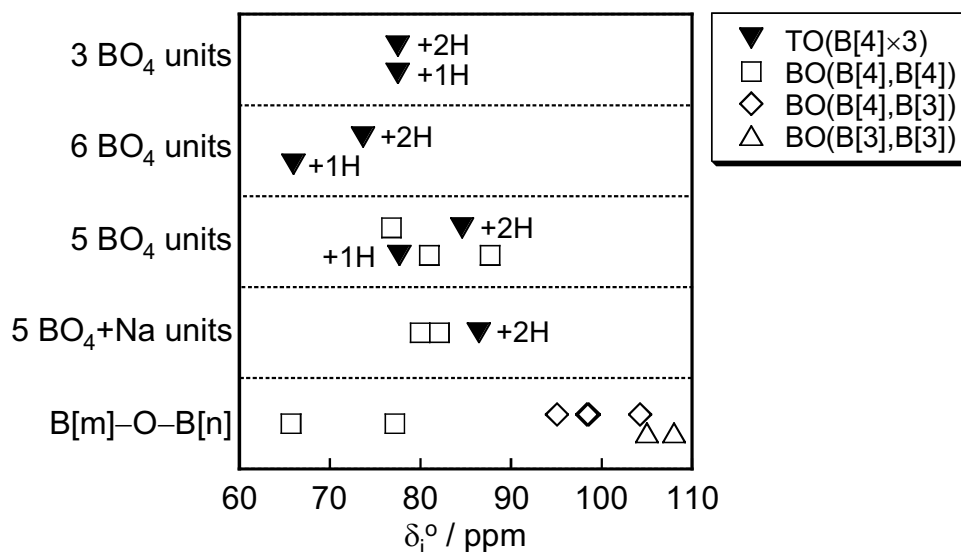


Figure 2: δ_i^O of tricluster oxygens and bridging oxygens in the various clusters

Quadrupole coupling constant C_q and asymmetry parameters η are shown in Figures 3 and 4, respectively. As shown in Fig. 3, C_q of $\text{TO}(\text{B}[4]_3)$ is larger than those of BOs in $\text{B}[4]\text{-O-B}[4]$, $\text{B}[4]\text{-O-B}[3]$ and $\text{B}[3]\text{-O-B}[3]$ bridges. In Fig. 4, η of $\text{TO}(\text{B}[4]_3)$ is smaller than those of BOs. Therefore, TOs and BOs may be identified by the combination of C_q and η .

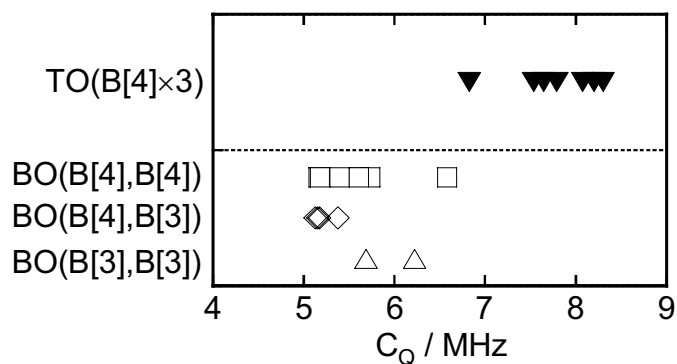


Figure 3: Quadrupole coupling constant C_Q of tricluster oxygens and bridging oxygens in the various clusters

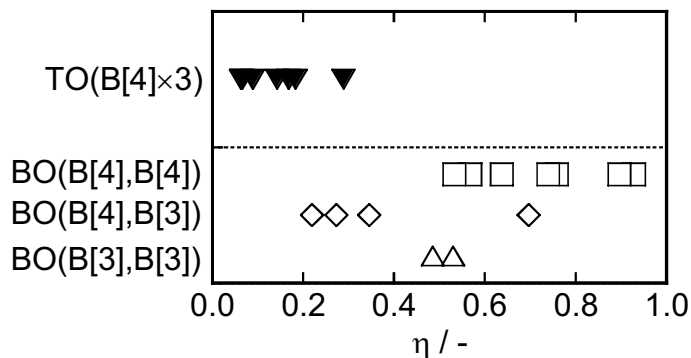


Figure 4: Asymmetry parameter η of tricluster oxygens and bridging oxygens in the various clusters

¹⁷O MQMAS NMR of Tricluster Oxygen

The peak positions in ¹⁷O MQMAS NMR spectrum reproduced from the above NMR parameters are shown in Figure 5. The peaks of tricluster and bridging oxygens in B–O–B bonds are narrowly distributed in the range of –60 ~ –90 ppm in isotropic dimension. In MAS dimension, however, the peak of TOs and BOs are located at different region, that is, the TO peaks are found at lower frequency (higher magnetic field) region and the BO peaks are at higher frequency region.

In the experimental ¹⁷O MQMAS NMR spectra reported by Wang et al. [17], BOs in B–O–B bridges are observed at $\delta_{\text{iso}} = -60 \sim -80$ ppm in isotropic dimension and $\delta_{\text{MAS}} = 90 \sim -30$ ppm, which is shown in Fig. 5. The peak positions estimated from the dimeric clusters for B–O–B bridges are located at the same region with the experiments [17]. TO(B[4]₃) in the cluster models appear at lower frequency region in MAS dimension than the experimental BOs in B–O–B bridges. Therefore, if unattributed component is found at lower frequency side of B–O–B component, it may be tricluster oxygen.

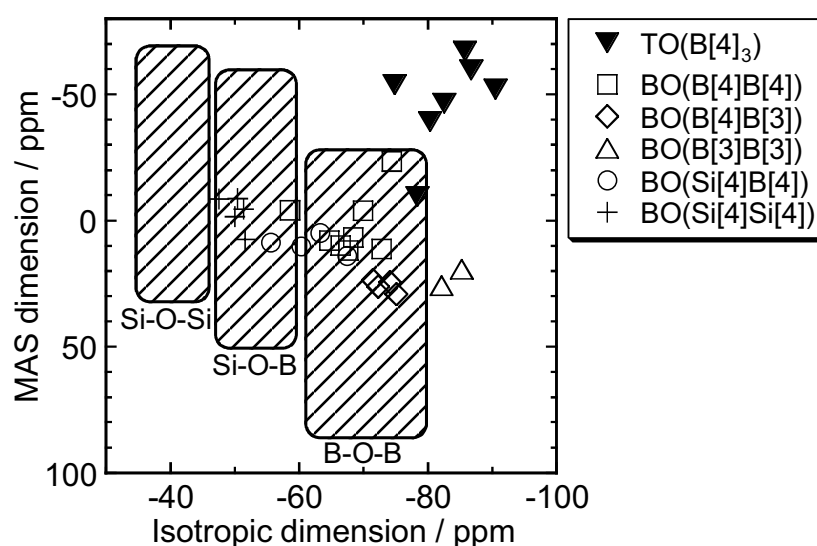


Figure 5: ¹⁷O MQMAS NMR peak positions of tricluster oxygens TO and bridging oxygens BO. The experimentally observed regions [17] are indicated by hatching.

In Fig. 5, the results of BOs in Si[4]–O–B[4] and Si[4]–O–Si[4] bridges are also shown, which are obtained from the dimeric clusters constructed from a borosilicate crystal, NaBSi₃O₈ [18]. Comparing the chemical shifts derived from MO calculations, BOs in Si–O–Si, Si–O–B and B–O–B bridges appear at the same region centering around 0 ppm in MAS dimension, and in isotropic dimension, however, they are located at different regions; BO(SiSi) = –50 ppm, BO(SiB) = –60 ppm and BO(BB) = –60 ~ –80 ppm. The order of the chemical shifts in isotropic dimension is consistent with the experimentally-given order, even though the absolute values of the chemical shifts are slightly different. The ¹⁷O MQMAS NMR peak positions of various borosilicate triclusters are plotted in Figure 6. TO(B[4]₃) in the cluster obtained by the geometry optimization is located at the same position with TO(B[4]₃) in the borate crystals, proving the validity of the cluster models. TOs surrounded by three boron atoms (a ~ d in Fig. 6) are narrowly distributed at the upper-right on the graph, that is, lower frequencies in both dimensions. With increasing the relative amount of trigonal B [3], the peak position shifts to the higher frequency sides in both dimensions. Furthermore, TOs coordinated by Si atoms (e ~ h in Fig. 6) appear at the lower-left among the TOs in Fig. 6, which is in the region of BOs in B–O–B

bridges. As for BOs, the experimentally-determined peak position shifts to the upper-left with increasing the number of Si atoms bonded to a BO. The peak shifts due to the Si contribution for BO and TO are the same in isotropic dimension but opposite in MAS dimension.

In the geometry optimizations, the local structure around the TOs was fixed. By elongating the bond lengths of TOs, the ^{17}O MQMAS NMR peaks commonly shifted to the lower frequency (right) side in isotropic dimension, while no significant shifts were observed in MAS dimension. The chemical shift in MAS dimension is probably sensitive to the bond angle, and further investigation on the bond angle dependency is, therefore, required. At least in this moment, the tricluster oxygen atoms surrounded by tetrahedral boron atoms might be identified by ^{17}O MQMAS NMR.

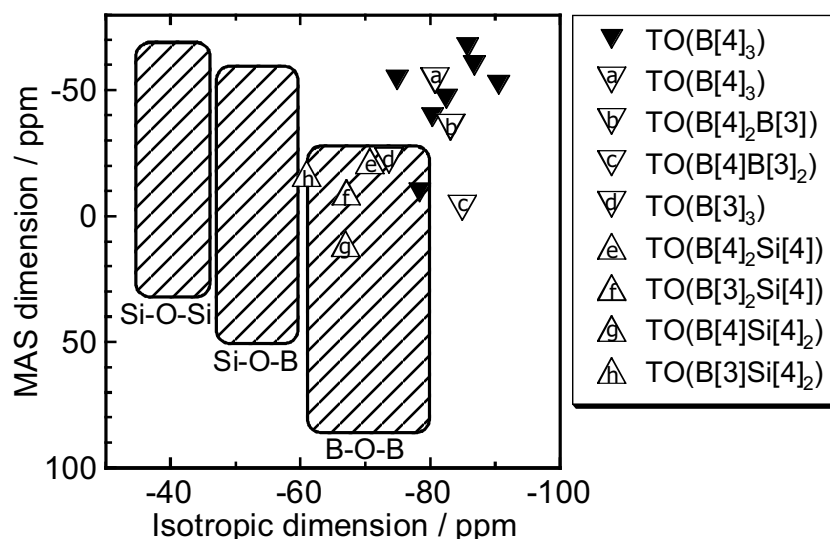


Figure 6: ^{17}O MQMAS NMR peak positions of tricluster oxygens.
Solid markers: cluster models constructed from borate crystals,
Open markers: cluster models from geometry optimization.
The experimentally observed regions [17] are indicated by hatching.

Conclusions

Cluster models containing tricluster oxygen atoms in the borosilicate system were constructed, and ^{17}O NMR parameters of the tricluster oxygen atoms were predicted by means of molecular orbital calculations. In the cluster models prepared from the borate crystals, the tricluster oxygen atoms surrounded by tetrahedral B[4] atoms showed similar isotropic chemical shifts δ_i^{O} as compared with the bridging oxygen atoms in B[4]–O–B[4] bridges. In quadrupole coupling constant C_Q and asymmetry parameter η , the tricluster and bridging oxygen atoms gave different values from each other. It was also the case in MQMAS NMR chemical shifts. The tricluster and bridging oxygen atoms appeared at the same region on isotropic dimension, and on MAS dimension, however, the tricluster oxygen atoms were located at the lower frequency region than the bridging oxygen atoms. The cluster models were also constructed by the geometry optimization of molecular orbital calculations. With increasing the number of Si and trigonal B[3] atoms bonded to the tricluster oxygen atoms, the ^{17}O MQMAS NMR peaks shifted to the higher frequency sides on both isotropic and MAS dimensions. Only the tricluster oxygen atoms surrounded by tetrahedral B[4] atoms might be identified by ^{17}O MQMAS NMR, which would be found at the lowest frequencies on both isotropic and MAS dimensions.

Acknowledgements

The authors would like to thank Profs. Xianyu Xue and Masami Kanzaki of Okayama University for their helpful advice in the MO calculations.

References

1. W.J. Dell, P.J. Bray, S.Z. Xiao, " ^{11}B NMR studies and structural modeling of $\text{Na}_2\text{O}-\text{B}_2\text{O}_3-\text{SiO}_2$ glasses of high soda content," *J. Non-Cryst. Solids*, 58 (1983), 1-16.
2. J.F. Stebbins, Z. Xu, "NMR evidence for excess non-bridging oxygen in an aluminosilicate glass," *Nature*, 390 (1997), 60-62.
3. P. Zhao, S. Kroeker, J.F. Stebbins, "Non-bridging oxygen sites in barium borosilicate glasses: Results from ^{11}B and ^{17}O NMR," *J. Non-Cryst. Solids*, 276 (2000), 122-131.
4. X. Xue, M. Kanzaki, "NMR Characteristics of Possible Oxygen Sites in Aluminosilicate Glasses and Melts: An ab Initio Study," *J. Phys. Chem.*, 103 (1999), 10816-10830.
5. J.D. Kubicki, M.J. Toplis, "Molecular orbital calculations on aluminosilicate tricluster molecules: Implications for the structure of aluminosilicate glasses," *Am. Mineral.*, 87 (2002), 668-678.
6. Y. Miura, H. Kusano, T. Nanba, S. Matsumoto, "X-ray photoelectron spectroscopy of sodium borosilicate glasses," *J. Non-Cryst. Solids*, 290 (2001), 1-14.
7. T. Nanba, Y. Miura, "Alkali Distribution in Borosilicate Glasses," *Phys. Chem. Glasses*, 44(3) (2003), 244-248.
8. T. Nanba, M. Nishimura, Y. Miura, "A theoretical interpretation of the chemical shift of ^{29}Si NMR peaks in alkali borosilicate glasses," *Geochim. Cosmochim. Acta*, 68(24) (2004), 5103-5111.
9. M. Urushihara, S. Sakida, T. Nanba, Y. Miura, "Theoretical Interpretation of ^{17}O NMR Spectra in Borosilicate Glasses," in Proceedings of Pacrim6 (S5-6), Maui, Hawaii, USA (2005).
10. C.T. Prewitt, R.D. Shannon, "Crystal structure of a high pressure form of B_2O_3 ," *Acta. Cryst.*, B24 (1968), 869-874.
11. A. Perloff, S. Block, "The Crystal structure of the Strontium and Lead Tetraborates, $\text{SrO} \cdot 2\text{B}_2\text{O}_3$ and $\text{PbO} \cdot 2\text{B}_2\text{O}_3$," *Acta Cryst.*, 20 (1966), 274-279.
12. J. Krogh-moe, "The Crystal Structure of Sodium Diborate $\text{Na}_2\text{O} \cdot 2\text{B}_2\text{O}_3$," *Acta. Cryst.*, B30 (1974), 578-582.
13. M.J. Frisch et al., GAUSSIAN 03, Gaussian, Inc., Pittsburgh, PA (2003).
14. J.R. Cheeseman, G.W. Trucks, T. A. Keith and M. J. Frisch, "A comparison of models for calculating nuclear magnetic resonance shielding tensors," *J. Chem. Phys.*, 104 (1996) 5497-5509.
15. J. Verhoeven, A. Dymanus, H. Bluysen "Hyperfine Structure of HD^{17}O by Beam-Maser Spectroscopy," *J. Chem. Phys.*, 15, (1969), 3330-3338.
16. S.H. Wang, et al., "Multiple-Quantum Magic-Angle Spinning and Dynamic-Angle Spinning NMR Spectroscopy for Quadrupolar Nuclei," *Solid State NMR*, 8 (1997), 1-16.
17. S. Wang, J.F. Stebbins, "Multiple-Quantum Magic-Angle Spinning ^{17}O NMR studies of Borate, Borosilicate, and Boroaluminate Glasses," *J. Am. Ceram. Soc.*, 82[6] (1999), 1519-1528.
18. D.E. Appleman, J.R. Clarl, "Crystal structure of reedmergnerite, a boron albite, and its relation to feldspar crystal chemistry," *Am. Mineral.*, 50 (1965), 1827-1850.